

# Recurrent connections between CA2 pyramidal cells

Kazuki Okamoto<sup>1</sup> & Yuji Ikegaya<sup>1,2,†</sup>

<sup>1</sup>Laboratory of Chemical Pharmacology, Graduate School of Pharmaceutical Sciences,  
The University of Tokyo, Tokyo, Japan

<sup>2</sup>Center for Information and Neural Networks, National Institute of Information and  
Communications Technology, Suita City, Osaka, Japan

†To whom correspondence should be addressed:

Yuji Ikegaya, PhD

Laboratory of Chemical Pharmacology

Graduate School of Pharmaceutical Sciences, The University of Tokyo

7-3-1 Hongo, Bunkyo-ku, Tokyo 113-0033, Japan

Tel.: +81-3-5841-4780; Fax: +81-3-5841-4786

Email: [yuji@ikegaya.jp](mailto:yuji@ikegaya.jp)

## 20    **Abstract**

21    Recurrent excitatory synapses are shown theoretically to play roles in memory storage  
 22    and associative learning, and such recurrent synapses are well described to occur in the  
 23    CA3 region of the hippocampus. Here, we report that the CA2 region also contains  
 24    recurrent excitatory monosynaptic couplings. Using dual whole-cell patch-clamp  
 25    recordings from CA2 pyramidal cells in mouse hippocampal slices under differential  
 26    interference contrast microscopic controls, we evaluated monosynaptic excitatory  
 27    connections. Unitary excitatory postsynaptic potentials occurred in 1.4% of 502 cell  
 28    pairs. These connected pairs were located preferentially in the superficial layer and  
 29    proximal part (CA2b) of the CA2 region. These results indicate that recurrent excitatory  
 30    circuits are dense in the CA2 region as well as in the CA3 region.

31

## 32 **Introduction**

33 Theoretical studies have suggested that reentrant positive-feedback excitation of the  
 34 neuronal network is critical for nonlinear information processing, including memory  
 35 storage, associative learning, and pattern separation/completion (Amari et al., 1996;  
 36 Hebb, 1949; Hopfield, 1982; Kohonen, 1998). The hippocampal CA3 region is one of  
 37 the candidate brain regions that anatomically contain self-associative excitatory  
 38 networks and functionally exert such information processing (Guzman et al., 2016;  
 39 MacVicar and Dudek, 1981; Miles and Wong, 1986; Nakazawa et al., 2004; Treves and  
 40 Rolls, 1994). However, only a few studies have directly measured monosynaptic  
 41 recurrent connections in the hippocampus (Deuchars and Thomson, 1996; Guzman et al.,  
 42 2016; Miles and Wong, 1986), particularly in the CA2 region (Mercer et al., 2012).

43         The CA2 region of the hippocampus is unique in terms of spatial representation  
 44 and social memory (Hitti and Siegelbaum, 2014; Mankin et al., 2015), but it has been  
 45 less investigated because it is not included in the classical tri-synaptic pathway and  
 46 because the CA2 region is anatomically small, which limits experimental access.  
 47 Notably, whether CA2 pyramidal cells are mutually excited at the monosynaptic level  
 48 remains controversial. Some reports suggest that the CA2 region contains recurrent  
 49 excitatory circuits (Lu et al., 2015) because CA2 neurons elaborate highly arborized  
 50 dendrites (Dudek et al., 2016) and because CA2 neurons can initiate sharp wave/ripple  
 51 oscillations (Oliva et al., 2016).

52         In the present study, we directly measured excitatory monosynaptic  
 53 connections between CA2 pyramidal cells using double whole-cell patch-clamp  
 54 recordings. We observed monosynaptic unitary excitatory postsynaptic potentials

(EPSPs) between 1.4% of the CA2 pyramidal cell pairs. The CA2-to-CA2 connections existed preferentially in the CA2b subarea and exhibited a preferential spatial direction.

## Results and Discussion

Recent histological studies have broadened the conventional definition (Lorente de Nó, 1934) of the CA2 region based on specific molecular expressions, such as those of G-protein signaling protein 14 (RGS14) and striatal-enriched protein tyrosine phosphatase (STEP) (Dudek et al., 2016; Kohara et al., 2014; Lein et al., 2005; Noguchi et al., 2017). We also confirmed that RGS14 immunoreactivity indicated the macroscopic location of the CA2 region in transverse slices of the hippocampus. At the single cell level, however, RGS14-positive cells were sparse near the CA1/CA2 and CA2/CA3 borders (Figure 1). This sparsity was found particularly in the ventral hippocampus. This salt-and-pepper distribution of RGS14-positive cells indicates that a significant number of non-CA2 pyramidal cells (presumably, CA1 or CA3 pyramidal cells) are present in the CA2 region.

We investigated recurrent CA2 connectivity by recording unitary EPSPs between two CA2 pyramidal cells. We visually targeted pyramidal cells using a differential interference contrast microscope. The recorded neurons were intracellularly filled with biocytin through patch-clamp pipettes and were then immunostained using an antibody against RGS14 or STEP (Figure 2A). A train of four action potentials was evoked at 20 Hz in one of the recorded cells, and the evoked membrane potentials were monitored for the other cells (Figure 2B). In the 502 pairs tested, we found 7 chemical synaptic connections and no electrical coupling; that is, the CA2-to-CA2 synaptic connection probability was 1.4%. The unitary EPSPs had a mean peak amplitude of

79 0.43  $\pm$  0.14 mV and a mean transmission failure rate of 54  $\pm$  24% (mean  $\pm$  SD of 7  
80 connections). Three of the 7 connections exhibited short-term depression in response to  
81 four presynaptic spikes (Figure 3). We also patched 108 CA3 pyramidal cell pairs and  
82 found 3 chemical synaptic connections (2.8%), whose unitary EPSPs had a mean peak  
83 amplitude of 0.75  $\pm$  0.54 mV and a mean failure rate of 45  $\pm$  22% (3 connections).  
84 These parameters of the CA3 pairs are similar to those reported in previous studies of  
85 CA3 connections (Guzman et al., 2016; Miles and Wong, 1986), and they did not differ  
86 significantly from those of the CA2 connections in the present study ( $P > 0.05$ ,  
87 Student's *t*-test).

88         During the whole-cell recordings, we measured the physical distances between  
89 the somata of two recorded cells in the images taken with a differential interference  
90 contrast microscope. The inter-soma distances were not correlated with the connection  
91 probability (Figure 4). This result appears similar to the previously reported spatial  
92 patterns of CA3 connectivity (Guzman et al., 2016) but is different from those of  
93 neocortical connectivity, in which more adjacent pairs had a higher probability of  
94 connections (Peng et al., 2017; Perin et al., 2011; Song et al., 2005). When considering  
95 the connectivity, however, one needs to consider the anatomical size of the CA2 region;  
96 the majority of CA2 cell pairs have inter-soma distances of less than 100  $\mu$ m; thus, we  
97 cannot rule out the possibility that this sampling restriction masked the distance  
98 dependence.

99         CA1 and CA3 pyramidal cells are heterogeneous along both transverse  
100 (Ishizuka et al., 1990; Lee et al., 2015; Lu et al., 2015; Sun et al., 2017) and radial axes  
101 (Kohara et al., 2014; Lee et al., 2014; Valero et al., 2015). Similar heterogeneity has also  
102 been reported in the CA2 region (Oliva et al., 2016). We thus investigated whether

103 CA2-to-CA2 connections are spatially biased in the CA2 stratum pyramidale. For one  
 104 of the 7 connections, we failed to accurately identify the relative loci of the recorded  
 105 cells in the RGS14-positive CA2 region. Thus, we analyzed the remaining 6 pairs. The  
 106 relative location of each recorded cell was determined in the CA2 stratum pyramidale,  
 107 which was rectangularly standardized according to the RGS14-positive or  
 108 STEP-positive areas (Figure 5A). In this cell map, we noticed two structural tendencies.  
 109 First, the directions from presynaptic cells to postsynaptic cells were spatially biased  
 110 (Figure 5B;  $V = 2.05$ ,  $P = 0.02$ ,  $n = 6$  pairs,  $V$ -test). A given CA2 pyramidal cell tended  
 111 to make a synaptic connection with a CA2 pyramidal cell that was more proximal to the  
 112 CA3 regions. This tendency suggests that compared to distal CA2 cells, more proximal  
 113 CA2 pyramidal cells receive more recurrent inputs from other CA2 pyramidal cells.

114 Second, the connected pairs were located preferentially in the superficial layer  
 115 and the proximal side of the CA2 region (Figure 5C). The difference between the  
 116 superficial and deep layers of the stratum pyramidale has not been well studied in the  
 117 CA2 region. A recent study demonstrated that the CA2 deep layer initiates sharp  
 118 wave/ripple oscillations (Oliva et al., 2016). Recurrent excitation is proposed as one of  
 119 the substrates of sharp wave/ripple generation (Traub et al., 1989), but our results  
 120 indicate that the recurrent connections of the CA2 pyramidal cells are nearly exclusively  
 121 located in the superficial layer. The generation of sharp waves/ripples is a complex  
 122 process, including dense recurrent circuits, timed interneuron activation (Stark et al.,  
 123 2014) and extrahippocampal controls (Buzsaki, 2015). The CA2 region may trigger  
 124 sharp waves/ripples independently of local recurrent excitation.

125 We found that the proximal CA2 (CA2b) subarea, but not the distal CA2  
 126 (CA2a) subarea, has dense recurrent connections, similar to the CA3 region. According

127 to the most recent definition (Dudek et al., 2016; Lein et al., 2005), the CA2b subarea  
 128 encompasses the stratum lucidum and receives monosynaptic inputs from the dentate  
 129 gyrus (Kohara et al., 2014; Sun et al., 2017); however, the unitary EPSP sizes are  
 130 smaller in CA2 pyramidal cells than in CA3 pyramidal cells (Sun et al., 2017). In  
 131 addition, CA2 pyramidal cells receive strong excitatory inputs from layer III neurons in  
 132 the entorhinal cortex (Chevalleyre and Siegelbaum, 2010). These extrahippocampal  
 133 inputs contribute to the unstable dynamics of CA2 neuronal activity (Lee et al., 2015;  
 134 Lu et al., 2015; Mankin et al., 2015). The CA3 network contains clustered circuit motifs  
 135 (Guzman et al., 2016). The neocortex also contains rich clustered connections (Peng et  
 136 al., 2017; Perin et al., 2011; Song et al., 2005). In CA2 pyramidal cells, we did not find  
 137 bidirectionally connected pairs. This may be because the numbers of pair recordings are  
 138 simply not enough.

139         A previous study reported a very low connection probability (0.22%) between  
 140 CA2 pyramidal cells (Mercer et al., 2012); however, this study did not identify CA2  
 141 pyramidal cells histologically using the CA2 cell markers (RGS-14 or STEP). Given  
 142 that CA2 pyramidal cells are sparse even in the CA2 pyramidal cell layer, the authors  
 143 may have underestimated the true CA2 connectivity. Another possibility is that they  
 144 might have focused more on the CA2a subarea, which was conventionally defined as  
 145 "the CA2 region". This sampling bias could also lead to an underestimation of the CA2  
 146 connectivity.

147         The CA2 region was reported to contain a higher density of GABAergic  
 148 interneurons than the CA1 or CA3 region (Leranth and Ribak, 1991; Mercer et al.,  
 149 2007). Interestingly, within the CA3 region, the CA3a subarea receives more inhibitory  
 150 inputs and has denser recurrent connectivity than the CA3b subarea (Sun et al., 2017).

151 These observations suggest similar circuit properties of the CA2b and CA3a subareas.  
152 The high density of recurrent excitatory connections may be counter-balanced by strong  
153 inhibitory inputs and maintain the excitatory-to-inhibitory balance in the CA2 local  
154 circuit.

155

## 156 **Methods**

### 157 *Animal experiment ethics*

158 Experiments were performed with the approval of the Animal Experiment Ethics  
159 Committee at the University of Tokyo (approval no. P29-9) and according to the  
160 University of Tokyo guidelines for the care and use of laboratory animals. Institute of  
161 Cancer Research (ICR) mice (SLC) were housed in cages under standard laboratory  
162 conditions (12 h light/dark cycle, ad libitum access to food and water). All efforts were  
163 made to minimize the animals' suffering and the number of animals used.

164

### 165 *Acute slice preparation*

166 Acute slices were prepared from the hippocampi of ICR mice (17-26 postnatal days).  
167 The mice were anesthetized with isoflurane and then decapitated. The brains were  
168 removed and placed in an ice-cold oxygenated solution consisting of (in mM) 222.1  
169 sucrose, 27 NaHCO<sub>3</sub>, 1.4 NaH<sub>2</sub>PO<sub>4</sub>, 2.5 KCl, 1 CaCl<sub>2</sub>, 7 MgSO<sub>4</sub>, and 0.5 ascorbic acid.  
170 The brains were sliced horizontally at a thickness of 400 μm using a VT1200S  
171 vibratome (Leica). The slices were allowed to equilibrate at room temperature for at  
172 least 0.5 h while submerged in a chamber filled with oxygenated aCSF consisting of (in  
173 mM) 127 NaCl, 26 NaHCO<sub>3</sub>, 1.6 KCl, 1.24 KH<sub>2</sub>PO<sub>4</sub>, 1.3 MgSO<sub>4</sub>, 2.4 CaCl<sub>2</sub>, and 10

174 glucose. The slices were mounted in a recording chamber and perfused at a rate of 1.5–3  
175 ml/min with oxygenated aCSF.

176

# 177 *In vitro electrophysiology*

178 All recordings were performed at 32–34°C. Whole-cell recordings were collected from  
179 up to four CA2 pyramidal cells using a MultiClamp 700B amplifier and a Digidata 1550  
180 digitizer controlled by pCLAMP10.6 software (Molecular Devices). Borosilicate glass  
181 pipettes (3–6 MΩ) were filled with a solution containing (in mM) 135 K-gluconate, 4  
182 KCl<sub>2</sub>, 0.3 EGTA, 10 HEPES, 10 Na<sub>2</sub>-phosphocreatine, 4 MgATP, 0.3 Na<sub>2</sub>GTP and 2.0  
183 biocytin. The signals were gained 10-fold, low-pass filtered at 1 kHz and digitized at 20  
184 kHz. The existence of synaptic connectivity was assessed by averaging 50 successive  
185 traces in which 4 spikes at 20 Hz were induced by current injection in presynaptic cells.

186

# 187 *Histology*

188 CA2 pyramidal cells were perfused intracellularly with 2 mM biocytin for whole-cell  
189 recordings. After the recordings, the slices were fixed for at least 20 h at 4°C in 0.1 M  
190 Na<sub>3</sub>PO<sub>4</sub>, pH 7.4, containing 3% (w/v) formaldehyde. The sections were incubated with  
191 2 µg/mL streptavidin-Alexa Fluor 594 conjugate and 0.2% Triton X-100 for 6 h,  
192 followed by incubation with 0.4% NeuroTrace 435/455 blue-fluorescent Nissl Stain  
193 (Thermo Fisher Scientific; N21479) overnight. The tissue sections were incubated  
194 subsequently with mouse primary antibodies for RGS-14 (NeuroMab; N133/21; 1:500)  
195 or STEP (Cell Signaling Technology; 4396S; 1:500) for 16 h at 4°C, followed by  
196 incubation with a secondary goat antibody to mouse IgG (Thermo Fisher Scientific;  
197 A-11001; 1:500) for 6 h at 4°C.

198

## 199 **References**

- 200 Amari S, Cichocki A, Yang HH. 1996. A new learning algorithm for blind signal  
201 separation. *Advances in neural information processing systems*. p 757-763.
- 202 Buzsaki G. 2015. Hippocampal sharp wave-ripple: A cognitive biomarker for episodic  
203 memory and planning. *Hippocampus* 25(10):1073-188.
- 204 Chevalleyre V, Siegelbaum SA. 2010. Strong CA2 pyramidal neuron synapses define a  
205 powerful disynaptic cortico-hippocampal loop. *Neuron* 66(4):560-72.
- 206 Deuchars J, Thomson AM. 1996. CA1 pyramid-pyramid connections in rat  
207 hippocampus in vitro: dual intracellular recordings with biocytin filling.  
208 *Neuroscience* 74(4):1009-18.
- 209 Dudek SM, Alexander GM, Farris S. 2016. Rediscovering area CA2: unique properties  
210 and functions. *Nat Rev Neurosci* 17(2):89-102.
- 211 Guzman SJ, Schlogl A, Frotscher M, Jonas P. 2016. Synaptic mechanisms of pattern  
212 completion in the hippocampal CA3 network. *Science* 353(6304):1117-23.
- 213 Hebb DO. 1949. *The organization of behavior; a neuropsychological theory*. New York,:  
214 Wiley. xix, 335 p. p.
- 215 Hitti FL, Siegelbaum SA. 2014. The hippocampal CA2 region is essential for social  
216 memory. *Nature* 508(7494):88-92.
- 217 Hopfield JJ. 1982. Neural networks and physical systems with emergent collective  
218 computational abilities. *Proc Natl Acad Sci U S A* 79(8):2554-8.
- 219 Ishizuka N, Weber J, Amaral DG. 1990. Organization of intrahippocampal projections  
220 originating from CA3 pyramidal cells in the rat. *J Comp Neurol* 295(4):580-623.
- 221 Kohara K, Pignatelli M, Rivest AJ, Jung HY, Kitamura T, Suh J, Frank D, Kajikawa K,  
222 Mise N, Obata Y and others. 2014. Cell type-specific genetic and optogenetic  
223 tools reveal hippocampal CA2 circuits. *Nat Neurosci* 17(2):269-79.
- 224 Kohonen T. 1998. The self-organizing map. *Neurocomput* 21:1-6.
- 225 Lee H, Wang C, Deshmukh SS, Knierim JJ. 2015. Neural Population Evidence of  
226 Functional Heterogeneity along the CA3 Transverse Axis: Pattern Completion  
227 versus Pattern Separation. *Neuron* 87(5):1093-105.
- 228 Lee SH, Marchionni I, Bezaire M, Varga C, Danielson N, Lovett-Barron M, Losonczy A,  
229 Soltesz I. 2014. Parvalbumin-positive basket cells differentiate among  
230 hippocampal pyramidal cells. *Neuron* 82(5):1129-44.
- 231 Lein ES, Callaway EM, Albright TD, Gage FH. 2005. Redefining the boundaries of the  
232 hippocampal CA2 subfield in the mouse using gene expression and

233 3-dimensional reconstruction. *J Comp Neurol* 485(1):1-10.

234 Leranth C, Ribak CE. 1991. Calcium-binding proteins are concentrated in the CA2 field  
235 of the monkey hippocampus: a possible key to this region's resistance to  
236 epileptic damage. *Exp Brain Res* 85(1):129-36.

237 Lorente de N6 R. 1934. Studies of the structure of the cerebral cortex. II. Continuation  
238 of the study of the ammonic system. *J Psychol Neurol* 46:113-177.

239 Lu L, Igarashi KM, Witter MP, Moser EI, Moser MB. 2015. Topography of Place Maps  
240 along the CA3-to-CA2 Axis of the Hippocampus. *Neuron* 87(5):1078-92.

241 MacVicar BA, Dudek FE. 1981. Electrotonic coupling between pyramidal cells: a direct  
242 demonstration in rat hippocampal slices. *Science* 213(4509):782-5.

243 Mankin EA, Diehl GW, Sparks FT, Leutgeb S, Leutgeb JK. 2015. Hippocampal CA2  
244 activity patterns change over time to a larger extent than between spatial  
245 contexts. *Neuron* 85(1):190-201.

246 Mercer A, Eastlake K, Trigg HL, Thomson AM. 2012. Local circuitry involving  
247 parvalbumin-positive basket cells in the CA2 region of the hippocampus.  
248 *Hippocampus* 22(1):43-56.

249 Mercer A, Trigg HL, Thomson AM. 2007. Characterization of neurons in the CA2  
250 subfield of the adult rat hippocampus. *J Neurosci* 27(27):7329-38.

251 Miles R, Wong RK. 1986. Excitatory synaptic interactions between CA3 neurones in the  
252 guinea-pig hippocampus. *J Physiol* 373:397-418.

253 Nakazawa K, McHugh TJ, Wilson MA, Tonegawa S. 2004. NMDA receptors, place  
254 cells and hippocampal spatial memory. *Nat Rev Neurosci* 5(5):361-72.

255 Noguchi A, Matsumoto N, Morikawa S, Tamura H, Ikegaya Y. 2017. Juvenile  
256 hippocampal CA2 region expresses aggrecan. *Front Neuroanat* 11:41.

257 Oliva A, Fernandez-Ruiz A, Buzsaki G, Berenyi A. 2016. Role of Hippocampal CA2  
258 Region in Triggering Sharp-Wave Ripples. *Neuron* 91(6):1342-1355.

259 Peng Y, Barreda Tomas FJ, Klisch C, Vida I, Geiger JRP. 2017. Layer-specific  
260 organization of local excitatory and inhibitory synaptic connectivity in the rat  
261 presubiculum. *Cereb Cortex* 27(4):2435-2452.

262 Perin R, Berger TK, Markram H. 2011. A synaptic organizing principle for cortical  
263 neuronal groups. *Proc Natl Acad Sci U S A* 108(13):5419-24.

264 Song S, Sjostrom PJ, Reigl M, Nelson S, Chklovskii DB. 2005. Highly nonrandom  
265 features of synaptic connectivity in local cortical circuits. *PLoS Biol* 3(3):e68.

266 Stark E, Roux L, Eichler R, Senzai Y, Royer S, Buzsaki G. 2014. Pyramidal  
267 cell-interneuron interactions underlie hippocampal ripple oscillations. *Neuron*  
268 83(2):467-80.

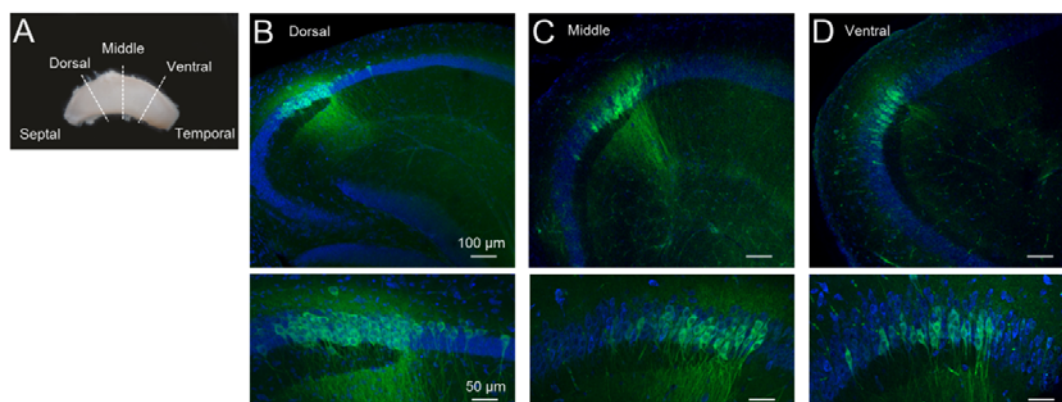
- 269 Sun Q, Sotayo A, Cazzulino AS, Snyder AM, Denny CA, Siegelbaum SA. 2017.  
 270 Proximodistal heterogeneity of hippocampal CA3 pyramidal neuron intrinsic  
 271 properties, connectivity, and reactivation during memory recall. *Neuron*  
 272 95(3):656-672 e3.
- 273 Traub RD, Miles R, Wong RK. 1989. Model of the origin of rhythmic population  
 274 oscillations in the hippocampal slice. *Science* 243(4896):1319-25.
- 275 Treves A, Rolls ET. 1994. Computational analysis of the role of the hippocampus in  
 276 memory. *Hippocampus* 4(3):374-91.
- 277 Valero M, Cid E, Averkin RG, Aguilar J, Sanchez-Aguilera A, Viney TJ,  
 278 Gomez-Dominguez D, Bellistri E, de la Prida LM. 2015. Determinants of  
 279 different deep and superficial CA1 pyramidal cell dynamics during sharp-wave  
 280 ripples. *Nat Neurosci* 18(9):1281-90.

281

## 282 **Acknowledgments**

283 We thank Dr. Segundo Jose Guzman, Dr. Vivien Chevaleyre, Dr. Rebecca Piskorowski,  
 284 and Dr. Takeshi Sakaba for their comments on the experiment. This work was  
 285 supported by Grants-in-Aid for Scientific Research (17K19441 & 18H05114) and by  
 286 the Human Frontier Science Program (RGP0019/2016). This work was conducted partly  
 287 as a program at the International Research Center for Neurointelligence (WPI-IRCIN) of  
 288 the University of Tokyo Institutes for Advanced Study at the University of Tokyo.

289

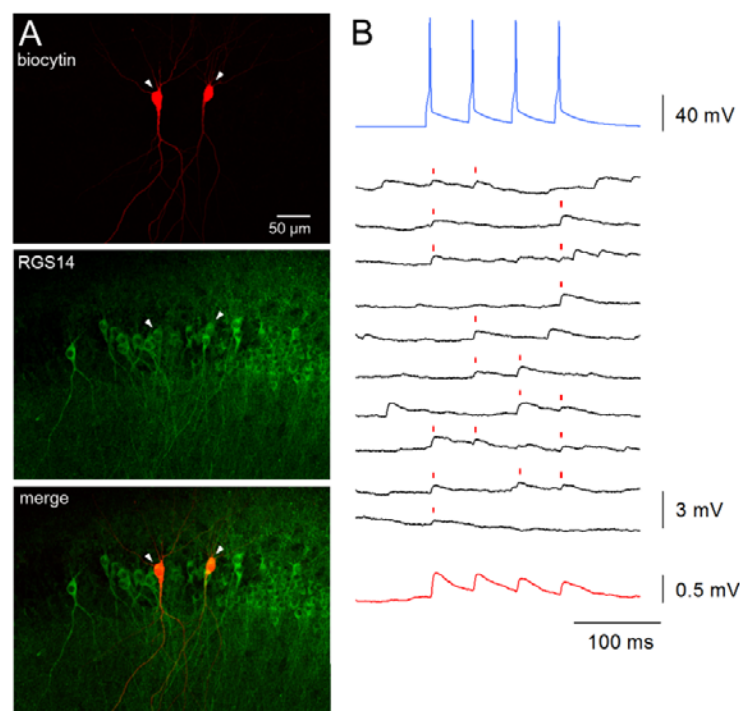


290

291

292 **Figure 1 | Distributions of CA2 pyramidal cells along the longitudinal axis of the**  
 293 **mouse hippocampus.** A) A whole hippocampus was sectioned transversely at the  
 294 dorsal, middle, and ventral areas, indicated by the broken white lines. **B-D)** The  
 295 transverse sections at the dorsal (B), middle (C), and ventral (D) areas were labeled with  
 296 an anti-RGS14 antibody (*green*, a CA2 marker) and NeuroTrace 435/455 Nissl Stain  
 297 (*blue*). The bottom photos are magnified images of the CA2 parts, indicating that the  
 298 CA2 borders next to the CA1 and CA3 regions are ambiguous because of the sparse  
 299 distribution of the CA2 pyramidal cells, particularly in the ventral hippocampus.

300



301

302

303 **Figure 2 | Monosynaptic recurrent connection of a CA2-CA2 pair.** A) *Top:*  
304 Confocal images of a synaptically connected pair of CA2 pyramidal cells that were  
305 filled with biocytin (*red*). *Middle:* The CA2 region was immunostained for RGS14  
306 (*green*). *Bottom:* RGS14 was expressed in the recorded cells. B) Unitary EPSPs of the  
307 connected pair. *Top:* Mean trace of a train of current injection-induced action potentials  
308 of the presynaptic cell (blue, averaged for 50 traces). *Middle:* Representative  
309 postsynaptic membrane responses recorded in the current-clamp mode for the  
310 successive trials (black). *Bottom:* an average of 50 recorded traces for the postsynaptic  
311 cell.

312

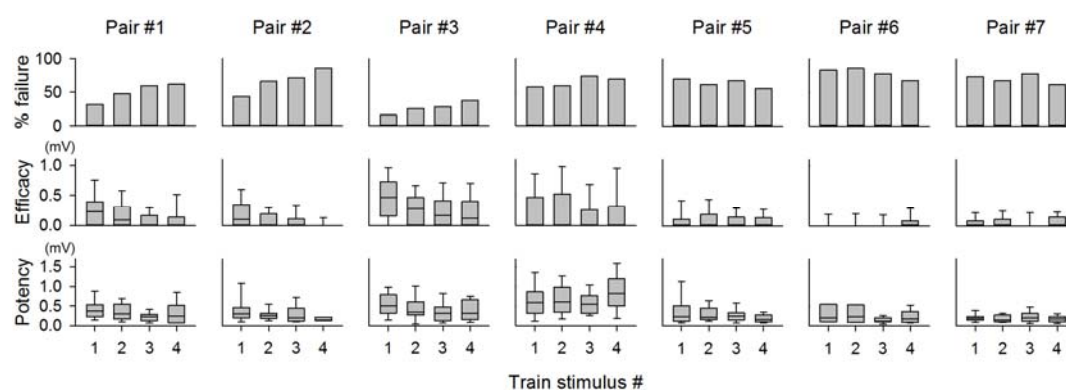
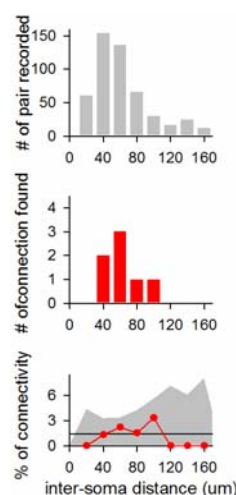


**Figure 3 | Unitary EPSP properties of all connected pairs.** *Top:* Percentages of synaptic failures in the responses to a presynaptic spike train (4 pulses at 20 Hz) for 7 connected pairs. Train stimuli were repeated 50 times. *Center:* Synaptic efficacies across the 50 trains (including failure events). *Bottom:* Synaptic potencies (without failure events).

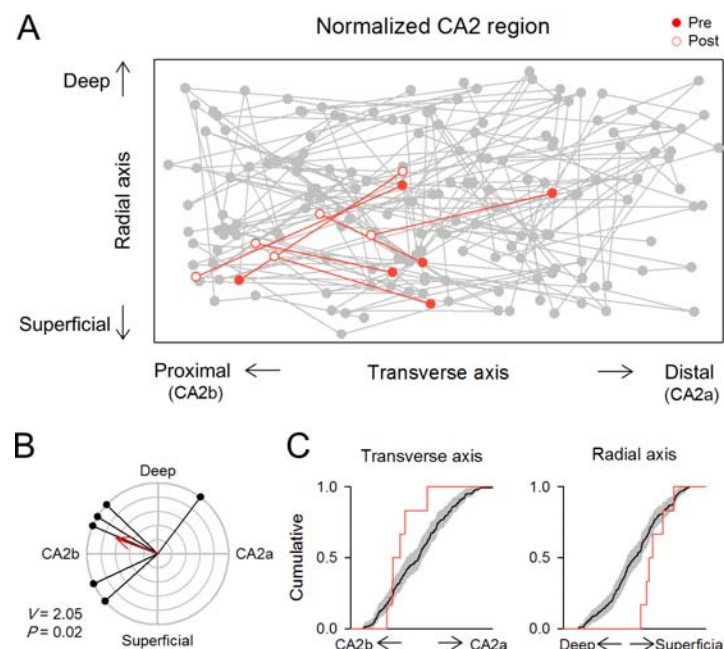


321

322

323 **Figure 4 | Lack of correlation of CA2-CA2 connections with their inter-cell**  
 324 **distances.** The top histogram indicates the distributions of the distances between the  
 325 centroids of the cell bodies of all recorded pairs. The center histogram indicates the  
 326 same distribution as the top, but for only the synaptically connected pairs. The bottom  
 327 graph plots the connection probabilities (*i.e.*, the center histogram divided by the top  
 328 histogram) as a function of the inter-soma distance (red). The black line is the mean  
 329 connection probability (1.4%). The gray area is the 95% confidence interval estimated  
 330 by 10,000 randomly resampled surrogates.

331

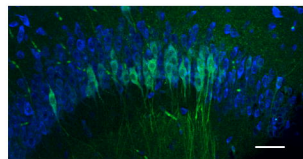
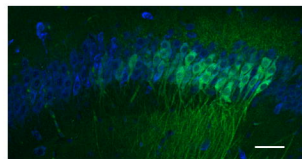
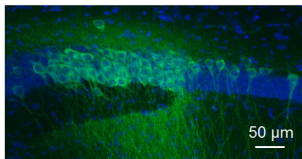
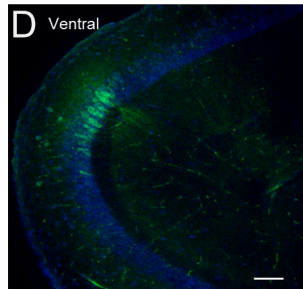
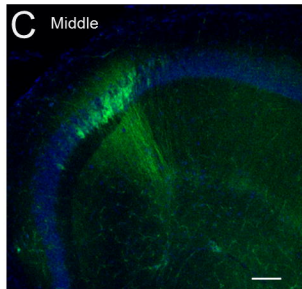
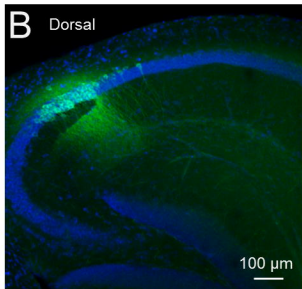
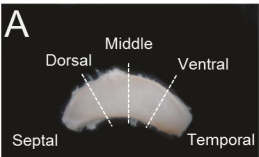


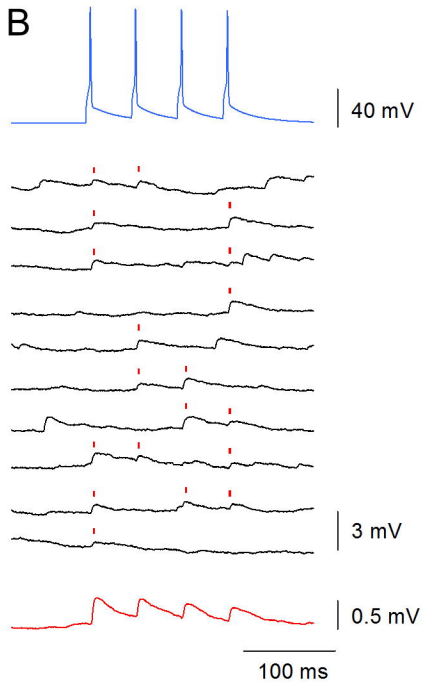
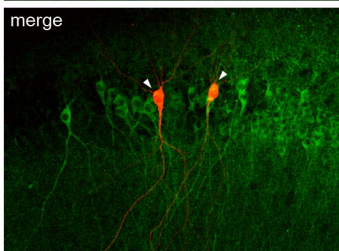
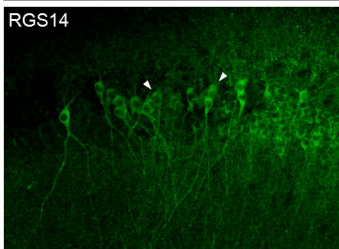
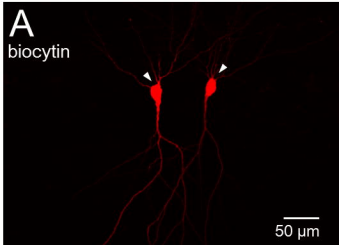
332

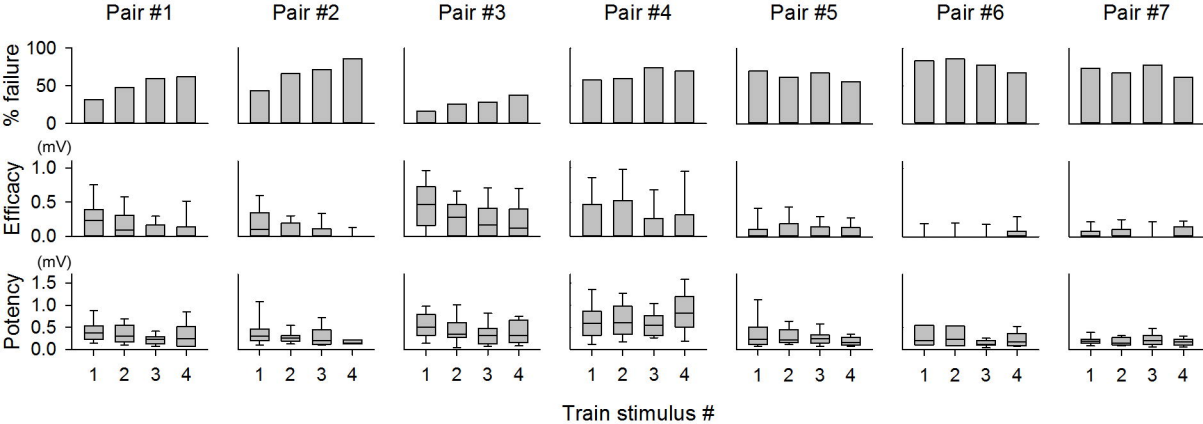
333

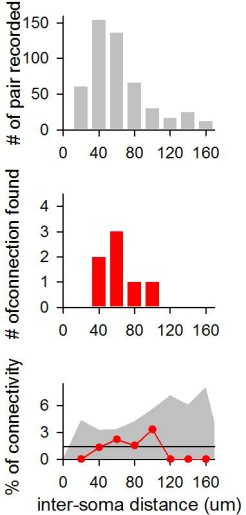
334 **Figure 5 | Spatial bias of CA2-CA2 connections.** **A)** The stratum pyramidale of the  
335 CA2 region was normalized as a rectangle according to RGS14-positive or  
336 STEP-positive areas. Gray dots and lines indicate the soma location of the recorded  
337 CA2 pyramidal cells and their potential connections (unconnected), respectively. Red  
338 lines represent the synaptic connections ( $n = 6$ ). Red filled and open circles indicate the  
339 soma location of the presynaptic and postsynaptic cells, respectively. **B)** A polar plot of  
340 the inter-soma directions of the synaptically connected pairs. Each black line indicates  
341 the direction from the soma of one presynaptic cell to the soma of its postsynaptic cell.  
342 The red arrow represents the mean vector of all 6 connected pairs.  $V = 2.05$ ,  $P = 0.02$ ,  
343  $V$ -test. **C)** Cumulative distributions of the midpoints between two soma locations of  
344 connected pairs (red line) and unconnected pairs (black line) along the transverse axis  
345 (left) and the radial axis (right). The gray areas indicate the 95% confidence intervals  
346 estimated by Kaplan-Meier method.

347





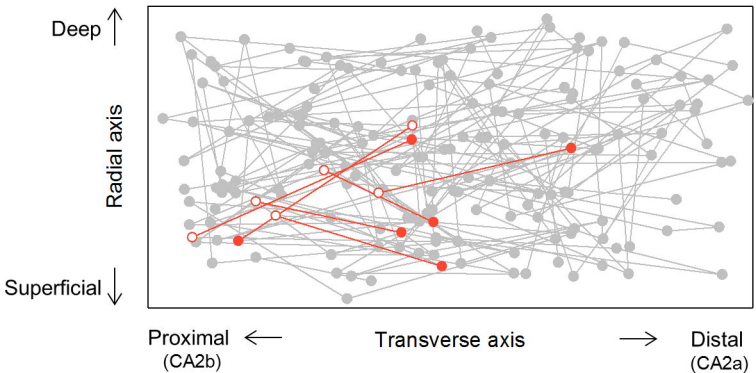
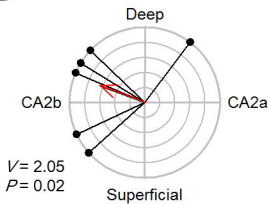




**A**

Normalized CA2 region

● Pre  
○ Post

**B****C**